

GeoResponder: Towards Building Geospatial LLMs for Time-Critical Disaster Response

Ahmed El Fekih Zguir
azguir@hbku.edu.qa

Qatar Center for Artificial Intelligence
Hamad Bin Khalifa University
Doha, Qatar

Ferda Ofli
fofli@hbku.edu.qa

Qatar Center for Artificial Intelligence
Hamad Bin Khalifa University
Doha, Qatar

Muhammad Imran
mimran@hbku.edu.qa

Qatar Center for Artificial Intelligence
Hamad Bin Khalifa University
Doha, Qatar

Abstract

Large Language Models excel at linguistic tasks but lack the inner geospatial capabilities needed for time-critical disaster response, where reasoning about road networks, continuous coordinates, and access to essential infrastructure such as hospitals, shelters, and pharmacies is vital. We introduce GeoResponder, a framework that instills robust spatial reasoning through a scaffolded instruction-tuning curriculum. By stratifying geospatial learning into different cognitive layers, we effectively anchor semantic knowledge to the continuous coordinate manifold and enforce the internalization of spatial axioms. Extensive evaluations across four topologically distinct cities and diverse tasks demonstrate that GeoResponder significantly outperforms both state-of-the-art foundation models and domain-specific baselines. These results suggest that LLMs can begin to internalize and generalize geospatial structures, pointing toward the future development of language models capable of supporting disaster response needs.

CCS Concepts

• **Computing methodologies** → **Natural language processing; Knowledge representation and reasoning**; • **Information systems** → **Geographic information systems**.

Keywords

Geospatial reasoning, Disaster response, Large language models, Critical infrastructure, OpenStreetMap

ACM Reference Format:

Ahmed El Fekih Zguir, Ferda Ofli, and Muhammad Imran. 2026. GeoResponder: Towards Building Geospatial LLMs for Time-Critical Disaster Response. In *Proceedings of Make sure to enter the correct conference title from your rights confirmation email (Conference acronym 'XX)*. ACM, New York, NY, USA, 11 pages. <https://doi.org/XXXXXXX.XXXXXXX>

1 Introduction

In the chaotic aftermath of a natural disaster, the efficacy of emergency response depends on the velocity of decision-making. First

responders are confronted with a deluge of critical inquiries, identifying the nearest accessible schools for shelter, verifying road connectivity for supply convoys, or locating hospitals within a serviceable radius [14, 18, 20, 22]. Although geospatial data for these tasks exists in platforms like OpenStreetMap (OSM), it remains locked behind complex Geographic Information Systems (GIS) requiring specialized expertise. This disconnect creates a dangerous “accessibility gap”: when data fluidity is most vital, the cognitive burden of translating natural language intent into rigid spatial queries becomes a bottleneck that compromises public safety.

Large Language Models (LLMs) offer a promising bridge across this gap by enabling responders to pose complex queries in natural language. However, while general-purpose LLMs possess high semantic fluency, they exhibit a profound deficit in geospatial reasoning (Figure 1). Recent “agentic” frameworks attempt to mitigate this by outsourcing spatial queries to external tools. While such agents remain indispensable for retrieving transient, real-time states, they are fundamentally brittle when tasked with complex spatial reasoning. Consider the query: “Find the nearest clinic to the shelter accessible without crossing the river.” A standard agent, relying on a general LLM to formulate tool parameters, will often fail to recognize the river as a topological barrier, retrieving a facility that is geometrically close but physically inaccessible. Although general LLMs may memorize that a specific hospital is in a specific city, they cannot reliably infer topology (how roads connect), metrics (the precise distance between two shelters), or orientation (the cardinal direction of an evacuation route) [3, 5, 11].

To address these limitations, we propose a shift from latent textual correlation to structured geospatial supervision. Rather than inferring proximity because two locations appear together in text, our approach teaches the model to verify their relationship through explicit coordinate-based rules. We introduce GeoResponder, a framework that translates deterministic GIS operations into natural language training signals, systematically bridging the gap between map data and language. Specifically, our methodology stratifies geospatial intelligence into three cognitive layers: **(i) Spatial grounding**, which anchors the model in static knowledge (e.g., resolving the entity “City Hospital” to its precise coordinates); **(ii) Spatial reasoning**, which enforces consistent logic for physical properties (e.g., calculating Haversine distance or verifying road intersections); and **(iii) Constraints-aware Spatial Retrieval**, a higher-order layer that challenges the model to solve complex tasks (e.g., identifying an evacuation route that bypasses blocked roads).

We empirically validate our approach across four topologically distinct urban environments: New York City, Paris, Christchurch, and Manila. These regions were selected to test generalization

Permission to make digital or hard copies of all or part of this work for personal or classroom use is granted without fee provided that copies are not made or distributed for profit or commercial advantage and that copies bear this notice and the full citation on the first page. Copyrights for components of this work owned by others than the author(s) must be honored. Abstracting with credit is permitted. To copy otherwise, or republish, to post on servers or to redistribute to lists, requires prior specific permission and/or a fee. Request permissions from permissions@acm.org.

Conference acronym 'XX, Woodstock, NY

© 2018 Copyright held by the owner/author(s). Publication rights licensed to ACM.

ACM ISBN 978-1-4503-XXXX-X/2018/06

<https://doi.org/XXXXXXX.XXXXXXX>

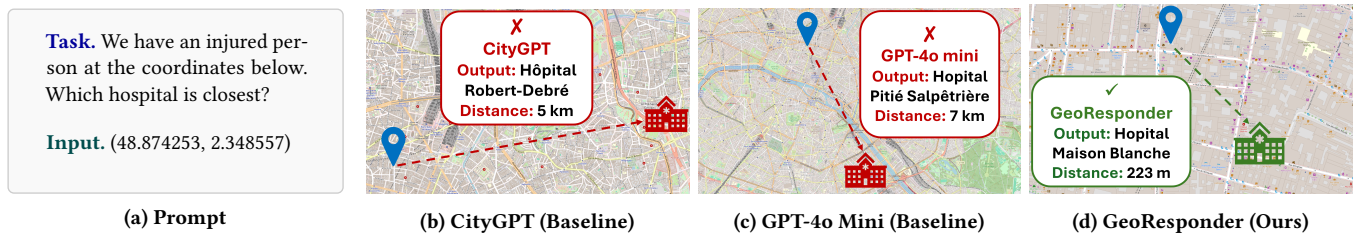


Figure 1: Qualitative comparison of SOTA models with GeoResponder.

across diverse road network structures, from the rigid orthogonal grids of the Global North to the irregular, organic layouts often found in the Global South. We train multiple foundation models, including Llama 3.1, Mistral 7B, and Qwen 8B, to assess cross-model robustness. Performance is benchmarked against strong geospatial baselines, like CityGPT [8], general-purpose foundation models, and inference-time strategies such as Chain-of-Thought (CoT) and few-shot prompting. Our results demonstrate that models trained on our geospatial representations consistently outperform all baselines, with the largest gains on tasks requiring multi-hop reasoning and constraint adherence.

2 Related Work

Recent studies have examined the extent to which LLMs can support geographic decision-making. Early evaluations by Bhandari et al. [3] showed that state-of-the-art models retain coarse geographic priors yet struggle with basic spatial understanding, including interpreting coordinates, resolving spatial prepositions, and judging relative positions between urban entities. Similar findings by Ji et al. [12] indicate that even high-performing models such as GPT-4 show inconsistent behavior on topological relations like containment or intersection. Broader evaluations in Roberts et al. [19] document failures in distance estimation, route reasoning, and geographic boundary inference. Embedding analyses from Gurnee and Tegmark [9] suggest that models may encode latent spatial information, but this structure remains too weakly organized to support reliable inference. These limitations mirror the challenge outlined in our introduction: general-purpose LLMs excel at semantic fluency but lack grounded spatial reasoning, particularly when queries require combining coordinates, geometry, and constraints.

To address these weaknesses, researchers have begun incorporating structured geospatial data into LLMs. Manvi et al. [17] augment model prompts with OSM metadata retrieved at inference time, improving accuracy on socioeconomic and demographic prediction tasks. Unlu [21] generate synthetic OSM question-answer pairs to fine-tune a small model for simple urban queries. Other work emphasizes spatially informed pretraining objectives. Li et al. [15] and Li et al. [16] design contrastive and coordinate-aware learning schemes that align textual descriptions with geographic context, improving entity linking and spatial classification. These approaches demonstrate the value of structured map-derived supervision, but they remain limited in scope. Most focus on POIs or city-level metadata and stop short of teaching models how to manipulate coordinates, derive distances, infer directions, or perform multi-step constraint-based retrieval.

Domain-specialized models also highlight the importance of structured spatial priors. K2 [6] and ERNIE-GeoL [10] integrate geoscience data and geographic graphs into pretraining to support scientific or cartographic applications. In the urban context, CityGPT [8] instruction-tunes an LLM using urban datasets to improve city-scale reasoning; we adopt this model as a strong baseline. Other systems such as LAMP [1] focus on POI-centric tasks like local recommendation. While these models incorporate valuable geographic information, most concentrate on coarse POI-level knowledge or textual summaries of cities. They do not provide the fine-grained spatial operators required to reason about coordinates, bounding boxes, filters, directions, or adjacency relations.

A separate research direction enhances LLMs through external GIS tools. GeoGPT [23] translates natural language into GIS operations (e.g. buffering), and Jiang et al. [13] uses a multi-agent framework where a controller LLM delegates sub-tasks to specialized solvers. These systems are effective when infrastructure is stable, but they depend on reliable tool access and precise parameterization—conditions that may not hold in fast-changing disaster settings. Our approach is complementary: by internalizing core spatial principles and learning structured GIS-aligned representations, we enable underlying models to perform consistent multi-step spatial reasoning both alongside external tools and in scenarios where tool use is constrained.

Finally, several non-LLM models provide strong performance on specific urban and road-network tasks. CityFM [2] and SARN [4] specialize in urban mapping, segmentation, or network extraction, but do not handle natural-language queries. They also do not attempt to teach a general LLM how to unify grounding, geometric operations, and multi-constraint inference. GeoResponder fills this gap by translating deterministic GIS operations into structured instruction-tuning signals. These signals span roads, POIs, bounding boxes, distances, directions, and category filters, and they are organized into a three-layer curriculum that strengthens grounding, geometric reasoning, and constraint-aware retrieval. This results in a model that can handle a broad suite of disaster-relevant spatial tasks rather than only road-based queries, and that consistently outperforms both general-purpose LLMs and domain-specific baselines such as CityGPT across multiple cities and network topologies.

3 Methodology

We argue that robust geospatial intelligence cannot emerge from unstructured textual pre-training alone; rather, it requires a scaffolded progression from static representation (e.g., real-world knowledge of road networks) to dynamic inference. To this end, we introduce

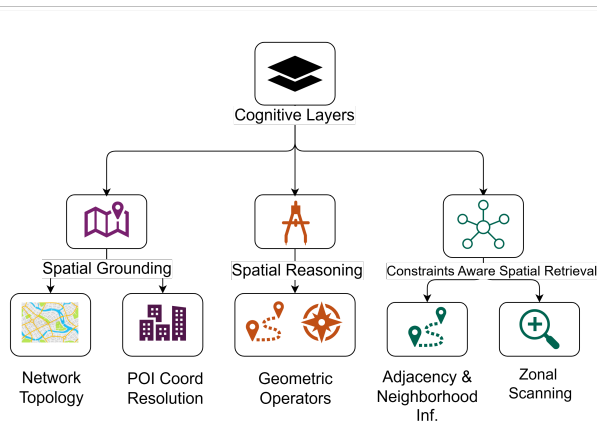


Figure 2: Visual Overview of the First 2 levels of the Cognitive Layers.

GeoResponder, a framework designed to construct spatial competency from first principles. Our approach begins by anchoring semantic entities, such as road segments and critical infrastructure, to the continuous coordinate manifold. This helps the model to establish a grounded mental map of the physical environment. Building upon this foundation, we enforce the internalization of geometric and topological knowledge to the model to derive spatial relationships. Finally, these primitives are synthesized to facilitate high-order reasoning by empowering the model to resolve the multi-step, constraint-heavy optimization problems characteristic of disaster response scenarios. The following sections detail our OSM preliminaries and representation formulations.

3.1 OpenStreetMap Structure and Notation

OpenStreetMap (OSM) is a collaborative geospatial database that represents the world using two core primitives: *nodes*, which are latitude–longitude points, and *ways*, which are ordered sequences of nodes forming linear features such as roads. Both rely on key–value tags (e.g., `highway=primary`, `name=ILam Road`) to encode semantic attributes. OSM also provides extensive coverage of *points of interest* (POIs) through tags such as `amenity`. In this work, we focus on *critical* POIs relevant to disaster response, including hospitals, schools, shelters, fuel stations, police stations, airports, and more.

A road segment s is defined as a contiguous portion of a way with consistent attributes. Using `osmnx`, we merge adjacent subpaths that share the same tags. Each segment has attributes $\text{Attr}(s)$ such as road type, speed limit, lane count, and length, and is represented by a polyline geometry $g = [\text{Coord}_1, \dots, \text{Coord}_m]$, where each $\text{Coord} = (lat, lon) \in \mathbb{R}^2$ denotes a WGS84 (EPSG:4326) coordinate. A named road R is the set of its constituent segments $\{s_1, \dots, s_n\}$ with aggregated attributes $\text{Attr}(R) = \text{aggregate}(\text{Attr}(s_1), \dots, \text{Attr}(s_n))$.

A POI is represented by a coordinate, a name, and a category `cat` (e.g., hospital, school, fuel). A bounding box (*bbox*) is an axis-aligned region defined by minimum and maximum latitude and longitude: $\text{bbox} = (lat_{\min}, lon_{\min}, lat_{\max}, lon_{\max}) \in \mathbb{R}^4$. A direction `dir` refers to one of the 8 cardinal directions (north, north-east, etc.), and a distance `dist` is expressed in meters.

3.2 Geospatial Representations

To enable language models to perform reliable geospatial reasoning and support complex disaster-oriented tasks, we design a set of structured geospatial representations that progressively build three layers of spatial intelligence (Figure 2). The first layer, **Spatial Grounding**, teaches the model to internalize a city’s geography by linking roads and critical POIs to the continuous coordinate space. This establishes a foundation where the model can interpret, reference, and reason about latitude–longitude pairs and associate them with real locations. The second layer, **Spatial Reasoning**, introduces fundamental operations over this grounded space, including distance estimation, direction inference, and basic topological checks. Once the model understands where things are and how spatial relationships behave, it must still solve real-world disaster queries that require filtering, constraint handling, and multi-step inference. We therefore introduce a third layer, **Constraint-aware Spatial Retrieval**, which trains the model to combine grounded knowledge and spatial operations to execute high-level tasks that involve multiple constraints and generalize to unseen scenarios.

3.2.1 Spatial Grounding. Through this layer, we provide the foundational factual knowledge and coordinate awareness upon which all higher-level geospatial reasoning is built. The goal of this layer is to make the model internalize the static structure of a city and link it to the continuous coordinate space. Concretely, the model must learn (i) the names and attributes of roads and POIs, and (ii) how these entities map to coordinates $\text{Coord} = (lat, lon)$ and vice versa. This establishes a bidirectional alignment between symbolic descriptions (road names, POI names, categories, attributes) and their physical representation in the underlying geographic space.

To construct this layer, we design a set of atomic representations clustered into two groups. The first group, *Network Topology Encoding*, captures the structure and attributes of the road network. It consists of three atomic representations: (i) *Road Attribute Retrieval* trains the model to map a road name R to its aggregated attributes $\text{Attr}(R)$. (ii) *Coordinate Localization* takes a coordinate Coord and requires the model to identify the road segment s for which Coord lies on its geometry $g = [\text{Coord}_1, \dots, \text{Coord}_m]$, returning both g and $\text{Attr}(s)$. This enforces a direct grounding between continuous coordinates and the road graph. (iii) *Segment Attribute Inference* uses the geometry g alone as input and trains the model to infer semantic properties such as road type, speed limit, or lane count, enabling it to understand spatial patterns directly from geometry.

The second Representation group, *POI Coordinate Resolution*, focuses on grounding critical infrastructure entities. (i) *POI Lookup* maps a POI name to its coordinate and category `cat`, while (ii) *Reverse POI Lookup* maps from a coordinate Coord back to the corresponding POI entity. Together, these representations give the model a structured grounding signal: it learns the set of city-specific entities, their attributes $\text{Attr}(\cdot)$, and how they are embedded in the continuous coordinate space. This layer forms the essential substrate on which subsequent spatial reasoning and complex disaster-oriented retrieval tasks are built.

3.2.2 Spatial Reasoning. Once the model has acquired spatial grounding and can map between city entities and the coordinate space, the next step is to introduce foundational operations that govern

spatial relationships. This layer trains the model to understand how coordinates relate to one another through basic geometric functions. By operating directly on coordinate pairs, the model develops an internal sense of spatial structure beyond memorized facts.

All atomic representations in this layer fall under a single representation group that we refer to as *Geometric Operators*. Within this group, we construct two core atomic representations. (i) *Distance Estimation* presents the model with a pair of coordinates and requires it to predict the geographic distance $\text{dist}(\text{Coord}_1, \text{Coord}_2)$ in meters. This teaches the model how spatial separation behaves in the latitude–longitude system and provides an implicit understanding of how far roads and POIs lie from one another. (ii) *Direction Inference* complements this by training the model to infer the relative position of Coord_2 with respect to Coord_1 , producing a cardinal direction dir such as north or west. Together, these representations equip the model with the basic geometric operators required to reason over continuous space and form the basis for more complex constraint-based spatial inference.

3.2.3 Constraint-aware Spatial Retrieval. To be useful in disaster settings, a model must solve geospatial tasks that combine grounding, geometric reasoning, filtering, and constraints. The third layer introduces representations that cover these tasks. These representations require the model to perform multi-step inference, integrate multiple forms of spatial information, and generalize beyond the atomic operations learned in earlier layers.

We cluster the atomic representations in this layer into two groups: *Zonal Scanning* and *Adjacency & Neighborhood Inference* (Figure 2). *Zonal Scanning* includes three bounding-box based atomic representations as follows: (i) *POI containment*: this representation lists all POIs whose coordinates fall within a given *bbox*, reinforcing the understanding of spatial clustering and inclusion. (ii) *Road containment*: this extends the reasoning to linear features, such as roads that contain at least one segment s whose geometry $g = [\text{Coord}_1, \dots, \text{Coord}_m]$ intersects the region defined by the *bbox*. This representation helps the model to reason not only about individual coordinates, but about the spatial extent of a polyline relative to a bounded query region. (iii) *Category Scan*: this representation increases the difficulty by adding a categorical filter, i.e., given a *bbox* and a category cat , the model must retrieve only the POIs of that type inside the region. These atomic representations simulate the kinds of map-window queries used routinely in GIS systems during disaster response (e.g., given the area of a wildfire, list all schools affected by it).

The second group, *Adjacency & Neighborhood Inference*, covers nearest-entity retrieval and directional neighborhood reasoning. (i) *Directional nearest road*, for a given coordinate Coord , contains the closest road segment lying in a specified cardinal direction dir , integrating distance estimation, directional reasoning, and projection onto the road network. (ii) *Nearest POI by category* represents situations when the need is to identify the nearest POI of a certain category. Both atomic representations require multi-hop inference over the grounded spatial knowledge acquired in earlier layers.

Together, these representations compel the model to move beyond memorized geospatial facts and simple geometric operations, enabling it to perform the kinds of structured, constraint-aware retrieval required in realistic disaster-response scenarios.

4 Experimental Setup

4.1 Dataset

To assess generalization, we select four cities: Christchurch (New Zealand), Manila (Philippines), Paris (France), and New York City (United States) from four continents. Christchurch and Manila are prone to disasters such as earthquakes and typhoons. Paris and New York City represent dense and globally recognizable urban environments with distinct spatial layouts and linguistic contexts.

Table 2 highlights the main attributes of each city. The POI distributions in Figure 6 shows Paris with the highest concentration of POIs, Christchurch the lowest, and Manila and New York City exhibit comparably dense and heterogeneous patterns. Quantitatively, Paris contains 4,062 critical POIs (about 38 per km^2), while Christchurch has 606. Manila and New York City show similar POI densities relative to their larger areas. Across all cities, the distribution of critical-infrastructure categories is similar (see Figure 7).

4.1.1 Training Data. For each city, we generate training data by instantiating the three cognitive layers of geospatial representations described in Section 3.2. All instances from these layers are then combined into a single city-specific dataset. In addition to the standard instruction-style formats, we also include a subset of multiple-choice (MCQ) variants to increase prompt diversity and better align with MCQ-style evaluation tasks.

Table 3 reports important stats of training data. Christchurch and Paris contain approximately 120–135k training instances, whereas Manila and New York City range between 500k and 600k. The majority of this increase arises from the spatial grounding layer, which scales with city area and POI density, producing substantially larger grounding datasets for Manila and New York compared to Paris and Christchurch.

Several representations require sampled coordinates (e.g., directional nearest-road, nearest POI by category), while others require sampled bounding boxes (e.g. POI containment). For coordinates, we use a density-aware strategy: the area of interest (the city) is divided into a uniform grid, and the number of points drawn per cell is proportional to the local density of road segments. Bounding boxes are sampled differently. We draw boxes with a maximum allowed area and enforce a minimum aspect-ratio constraint to avoid degenerate, overly thin regions. To ensure coverage of empty or sparsely populated zones, we also include a controlled number of *empty* boxes that contain no POIs or road segments, which helps the model learn to distinguish between populated and non-populated spatial windows.

4.2 Evaluation Tasks

To comprehensively assess geospatial reasoning performance, we evaluate our models on a suite of downstream tasks that are both challenging and directly relevant to disaster response. Table 1 lists all evaluation tasks, organized by the cognitive layer they probe and by the underlying geospatial operation they correspond to. For clarity, the table also specifies the input–output notation for each task and provides a short disaster-response scenario illustrating its real-world relevance.

We report results for both multiple-choice (MCQ) and free-form versions of tasks. The MCQ format supplies four candidate answers

Table 1: Taxonomy of evaluation tasks grouped by Spatial Grounding, Spatial Reasoning, and Spatial Retrieval. Text colors indicate the cognitive layer.

Cognitive Layer	Representation Group	Task Name	Notation (Input - Output)	Disaster Response Example	Metric
1. Spatial Grounding <i>(Static Knowledge)</i>	Network Topology Encoding	Rev. Road Attr. Lookup	$Coord(\in Seg) \rightarrow Attr$	Check if a road segment supports heavy rescue vehicles.	Acc, MAPE, F1
		Rev. Road Lookup	$Coord(\in Seg) \rightarrow Road$	Retrieve street name to guide ground teams.	Acc
	POI Coordinate Resolution	POI Lookup	$POI \rightarrow Coord$	Convert "Fire at City Hospital" into coordinates.	F1
		Rev. POI Lookup	$Coord \rightarrow POI$	Identify a collapsed facility from aerial coordinates.	Acc
2. Spatial Reasoning <i>(Geometric Logic)</i>	Geometric Operators	Distance Est.	$(Coord_A, Coord_B) \rightarrow Meters$	Determine if a supply truck can reach a shelter with fuel.	MAPE
		Direction Inf.	$(Coord_A, Coord_B) \rightarrow Dir.$	Determine a safe helicopter heading to avoid smoke.	F1
3. Constraints Aware Spatial Retrieval <i>(Constraint Inf.)</i>	Zonal Scanning	Road Containment	$BBox \rightarrow \{Roads_{in}\}$	List roads within the predicted flood polygon.	F1
		Road Exclusion	$BBox \rightarrow \{Roads_{out}\}$	Identify staging areas outside a chemical spill.	-
		POI Containment	$BBox \rightarrow \{POIs_{in}\}$	List schools located within the earthquake area.	F1
		POI Exclusion	$BBox \rightarrow \{POIs_{out}\}$	Identify shelters outside of the disaster area.	-
		Category Scan	$(BBox, Cat) \rightarrow \{POI_{list}\}$	Retrieve all gas stations in a grid sector to secure fuel supply.	F1
	Adjacency & Neighborhood Inf.	Nearest POI by Cat	$(Coord, Cat) \rightarrow POI$	Locate the nearest pharmacy to a location.	Acc
		Neighbor POI	$POI_A \rightarrow POI_B$	Find the closest hospital to the school.	-
		Nearest Road (POI)	$POI \rightarrow Road_{nearest}$	Find the nearest road access point near an evacuation camp.	-
		Dir. Nearest Road	$(Coord, Dir) \rightarrow Road$	Find the nearest safe road north of some coordinates.	Hit@K, Acc@1km, MRR
		Nearest Road	$Coord \rightarrow Road$	Identify the nearest road to some coordinates.	Hit@K, Acc@1km, MRR

Table 2: City-level OpenStreetMap statistics.

Statistic	Christch.	Paris	Manila	New York
Continent	Oceania	Europe	Asia	N. America
City area (km ²)	295	105	619	778
Road segments	23,773	17,681	124,275	135,625
Unique roads (name)	3,980	3,865	11,514	7,776
Total road length (km)	4,868	2,634	12,485	20,619
Road length density (km/km ²)	16.5	25.1	20.2	26.5
# of POIs (Critical Infrastructure)	606	4,062	7,015	5,586
POI density (per km ²)	2.1	38.7	11.3	7.2

Table 3: Training data size across layers for each city.

Cognitive layer	Christch.	Paris	Manila	New York
Spatial grounding	100,919	87,517	529,589	567,402
Spatial reasoning	4,800	4,800	4,800	4,800
Const.-aware spatial retrieval	28,566	28,010	32,045	48,530
Total	134,285	120,327	566,434	620,732

and tests recognition under constrained choices, while the free-form

setting requires the model to generate the correct output without any options provided, making it substantially more difficult.

To further test the limits of generalization, we introduce a set of out-of-distribution (OOD) tasks representing geospatial operations that are never seen during training. These include *POI Exclusion*, *Road Exclusion*, *Neighbor POI Identification*, and *POI-to-Nearest-Road*. When evaluated, each OOD task is framed within a realistic disaster-response scenario (see the prompt example in Figure 10). This setup allows us to measure whether the model can transfer its learned spatial reasoning capabilities to entirely novel geospatial queries.

4.3 Evaluation Metrics

We employ a diverse set of evaluation metrics strictly aligned with the output modality of each geospatial task. While standard accuracy suffices for multiple-choice questions, we evaluate free-form geometric and retrieval tasks using specialized rank-aware and distance-based measures. For distance estimation, we report Mean Absolute Percentage Error (MAPE), whereas retrieval tasks (e.g., *Nearest Road*) are assessed via *Acc@1km*—verifying if predictions lie within a 1 km geodesic radius—and *Hit@k*, formally defined as $Hit@k = \frac{1}{n} \sum_{i=1}^n 1\{\hat{r}_i \in G_i^{(k)}\}$, alongside Mean Reciprocal Rank (MRR). For directional variants, these metrics are averaged across all cardinalities. Finally, set-valued generation tasks require

Algorithm 1 F1 Evaluation for POI Lookup

Require: Predicted coordinate sets $\{\hat{C}_i\}$, ground-truth sets $\{C_i\}$, distance threshold τ

- 1: **for** $i = 1$ to N **do**
- 2: $G \leftarrow$ set of ground-truth coordinates in C_i
- 3: $n_{\text{correct}} \leftarrow 0$
- 4: **for** each predicted coordinate $\hat{c} \in \hat{C}_i$ **do**
- 5: $(g^*, d^*) \leftarrow \arg \min_{g \in G} \text{GEODESICDISTANCE}(\hat{c}, g)$
- 6: **if** $d^* \leq \tau$ **then**
- 7: $n_{\text{correct}} \leftarrow n_{\text{correct}} + 1$
- 8: $G \leftarrow G \setminus \{g^*\}$ \triangleright greedy one-to-one match
- 9: **end if**
- 10: **end for**
- 11: $p_i \leftarrow n_{\text{correct}} / |\hat{C}_i|$
- 12: $r_i \leftarrow n_{\text{correct}} / |C_i|$
- 13: $f_i \leftarrow \frac{2p_i r_i}{p_i + r_i}$ \triangleright F1 score
- 14: Record f_i
- 15: **end for**
- 16: **return** mean F1 across all examples

overlap-based scoring: *Road Containment* utilizes exact-intersection F1 scores, while *POI Lookup* adopts a greedy one-to-one geodesic matching protocol (Algorithm 1) that validates predictions falling within a 150 m threshold of ground-truth coordinates.

4.4 Baselines

We compare GeoResponder against strong open-source instruction-tuned baselines—Qwen 3 8B, LLaMA 3.1 8B, Mistral 7B v0.3, and the proprietary GPT-4o Mini. All models are evaluated under two prompting regimes: (i) *Direct Prompting*, using concise task-specific instructions; and (ii) *Geo Prompt Fusion*, which integrates chain-of-thought reasoning, structured OSM-based contextual grounding (similar to [17]), and QSF-based retrieval of geographically proximate few-shot exemplars [7].

For *multiple-choice* tasks, we additionally benchmark against the geospatial LLM CityGPT [8] using their SFT variant. We reproduce their Qwen 2.5 7B model using the hyperparameters reported in their paper. Although CityGPT provides training data for several cities, it does not release datasets for two of our evaluation cities (Christchurch and Manila), so we train it only on Paris and NYC.

5 Evaluation and Results

5.1 In-Distribution MCQ Tasks

Table 4 reports results on the in-distribution MCQ tasks. In Paris and New York, we additionally compare GeoResponder against the geospatially trained CityGPT baseline.

CityGPT performs well on simpler grounding tasks such as POI Lookup and Road Containment, but its accuracy drops sharply on tasks that depend on modeling the continuous coordinate space or reasoning over bounded regions (Reverse POI Lookup, POI Containment, Nearest-POI-by-Category, Category Scan). These failures highlight its limited understanding of fine-grained spatial relationships despite being pre-trained on OSM-derived data.

GeoResponder, particularly the Mistral variant, achieves large gains across all tasks and all cities. Improvements over CityGPT typically exceed +100% and often surpass +150%, with the largest margins appearing precisely on the tasks where CityGPT struggles. This demonstrates GeoResponder’s stronger grounding in spatial neighborhoods, containment logic, and category-filtered retrieval.

Absolute accuracy varies systematically by city. Manila and New York, which cover larger areas and exhibit high POI diversity, yield lower scores on POI Lookup and Reverse POI Lookup due to increased spatial ambiguity and denser candidate sets. Christchurch and Paris show higher accuracy on grounding-oriented tasks, consistent with their smaller spatial extents and more concentrated POI distributions. Overall, these results confirm that (i) structured geospatial representations are essential for reliable spatial reasoning, (ii) GeoResponder generalizes across cities with diverse spatial scales, and (iii) task difficulty correlates strongly with city size, POI density, and the geometric complexity of the underlying operation.

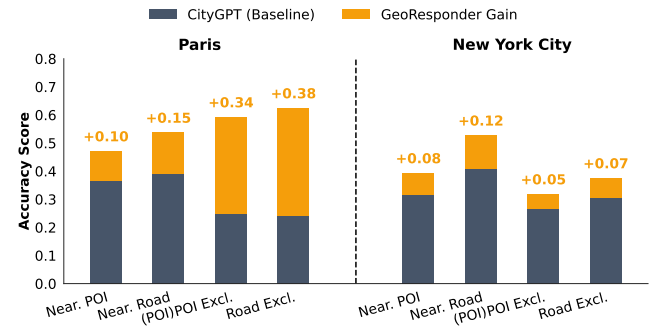


Figure 3: Out-of-distribution disaster tasks: stacked comparison between CityGPT performance (grey) and the absolute improvement achieved by GeoResponder–Mistral (yellow).

5.2 Road-network reasoning on free-form tasks

Table 5 evaluates whether GeoResponder’s three-layer curriculum yields reliable free-form geospatial reasoning. Results are reported across four cities and three task groups aligned with our cognitive layers: (i) *Nearest Road Retrieval*, (ii) *Geometric Operators* (distance, direction), and (iii) *Reverse Road Attribute and Name Lookup*. For each city, we compare base instruction-tuned models, their Geo Prompt Fusion variants, and all GeoResponder backbones.

Directly prompted LLaMA, Mistral, and Qwen models perform poorly across all settings: nearest-road Hit@1 is near zero, distance MAPE remains high, directional F1 is low, and both road-name and attribute extraction rarely succeed. Geo Prompt Fusion improves these baselines by adding chain-of-thought, OSM context, and geographically proximate few-shot examples, raising Acc@1km to the 0.2–0.4 range and yielding modest gains in segment metadata inference. However, performance remains inconsistent, especially in Paris, Manila, and New York, indicating that inference-time prompting alone cannot substitute for grounded spatial representations.

GeoResponder closes this gap substantially. Because its curriculum explicitly grounds entities in the coordinate manifold (Layer 1),

Table 4: Performance across six geospatial tasks for GeoResponder and CityGPT. Best GeoResponder values (Mistral) are bold.

City	Model	POI Lookup	Rev. POI Lookup	Road Containment	POI Containment	Nearest POI by Cat	Category Scan
Christchurch	GeoResponder (LLaMa)	0.5	0.564	0.574	0.694	0.7435	0.689
	GeoResponder (Mistral)	0.78	0.637	0.637	0.793	0.856	0.77
	GeoResponder (Qwen)	0.472	0.317	0.536	0.565	0.4	0.561
Paris	CityGPT	0.316	0.219	0.291	0.223	0.24	0.259
	GeoResponder (LLaMa)	0.624	0.425	0.601	0.583	0.467	0.505
	GeoResponder (Mistral)	0.75	0.62	0.68	0.685	0.723	0.633
	GeoResponder (Qwen)	0.46	0.25	0.456	0.482	0.326	0.345
	Best GeoResponder vs CityGPT (%)	0.75	0.62	0.68	0.685	0.723	0.633
Manila	GeoResponder (LLaMa)	0.488	0.43	0.512	0.509	0.47	0.564
	GeoResponder (Mistral)	0.497	0.5	0.576	0.576	0.562	0.595
	GeoResponder (Qwen)	0.464	0.419	0.5	0.508	0.432	0.503
New York City	CityGPT	0.33	0.247	0.31	0.23	0.265	0.274
	GeoResponder (LLaMa)	0.46	0.45	0.6	0.61	0.6	0.61
	GeoResponder (Mistral)	0.517	0.568	0.685	0.714	0.749	0.723
	GeoResponder (Qwen)	0.437	0.394	0.602	0.632	0.476	0.614
	Best GeoResponder vs CityGPT (%)	0.517	0.568	0.685	0.714	0.749	0.723
		+57	+130	+121	+210	+183	+164

internalizes geometric operators (Layer 2), and practices constraint-based retrieval (Layer 3), it achieves robust free-form reasoning without specialized prompts. Across all cities, the strongest GeoResponder variant improves nearest-road Hit@1 by +146%–+657%, directional Hit@1 by +163%–+237%, and reduces distance MAPE by 80%–95%. Road-name accuracy rises from below 0.16 in all baselines to 0.47–0.79, while speed and lane F1-scores reach 0.39–0.68 and 0.43–0.65. Gains are largest in Manila and New York, where large and irregular road networks impose significant generalization challenges. Among backbones, Mistral performs best overall, with LLaMA close behind; Qwen is strong primarily in Manila and New York. The main remaining difficulty is segment-length estimation in Paris, reflecting the complexity of dense European urban geometry.

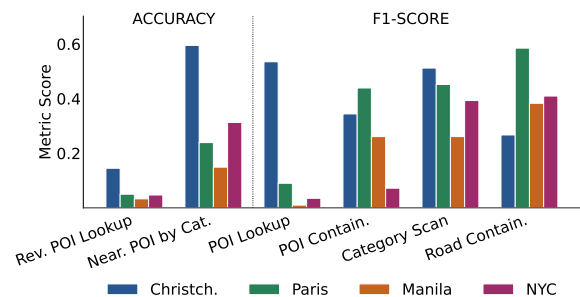
5.3 Out-of-distribution MCQ tasks

Figure 3 reports accuracy on the out-of-distribution MCQ tasks in Paris and New York City. These evaluations probe whether models can transfer the grounded and geometric competencies learned to spatial queries and task formats not seen during training.

GeoResponder (Mistral) achieves consistent gains across all OOD tasks, with the largest improvements on POI Exclusion and Road Exclusion. Both tasks require multi-step spatial filtering—identifying which entities lie *outside* a specified region—thus stressing the model’s ability to combine zonal scanning with fine-grained coordinate reasoning. The strong performance suggests that GeoResponder’s constraint-aware retrieval layer generalizes effectively even when the task logic differs from the atomic representations used during training.

CityGPT exhibits notably lower accuracy on these exclusion-based tasks, especially those involving precise coordinate comparisons. Its performance trends mirror the challenges observed in

the in-distribution evaluation, indicating that it generalizes less reliably to spatial structures that deviate from its training format. By contrast, GeoResponder maintains robust accuracy across both cities and task types, highlighting its stronger capacity to transfer spatial reasoning beyond the distributions and representations it was explicitly trained on.

**Figure 4: In-distribution non-MCQ bar distribution.**

5.4 In-Distribution Non-MCQ Tasks

Figure 4 reports GeoResponder (Mistral) performance on non-MCQ tasks across all four cities. Reverse POI Lookup emerges as the most challenging task: mapping from the continuous space to a discrete entity is inherently difficult and becomes increasingly ambiguous as POI density grows. Similarly, POI Lookup accuracy degrades in dense cities like Manila and NYC, confirming that large, crowded candidate spaces impede retrieval.

Performance on the remaining tasks is more consistent. POI Containment and Category Scan exhibit moderate variation across

Table 5: Performance evaluation across eight tasks and cities. The final rows compare the best GeoResponder against the strongest baseline. Darker shades indicate superior performance.

City	Model	Nearest Road						Geometric Operators		Rev. Road Attr. and Name Lookup				
		Standard			Directional			Dist	Dir	Road	Length		Speed	Lanes
		Hit@1	Acc@1km	MRR	Hit@1	Acc@1km	MRR	MAPE ↓	F1	Acc	MAPE ↓	Acc@30%	F1	F1
Christchurch	LLaMa 3.1 8B	0	0.013	0.002	0	0	0	0.695	0.14	0.002	2.7821	0.114	0	0.2332
	Mistral 7B v0.3	0.002	0.017	0.001	0.027	0.027	0.018	1.33	0.03	0	8.3	0.016	0	0.1858
	Qwen3 8B	0	0.004	0.001	0.002	0.002	0.002	0.678	0.03	0.001	1.6582	0.235	0	0.2334
	GeoPromptFusion (LLaMa)	0.16	0.44	0.218	0.134	0.237	0.165	0.4429	0.19	0.064	0.9429	0.289	0.1772	0.1864
	GeoPromptFusion (Mistral)	0.169	0.595	0.252	0.092	0.124	0.101	0.6697	0.06	0.025	1.0249	0.2683	0.1869	0.2829
	GeoPromptFusion (Qwen)	0.23	0.676	0.321	0.129	0.265	0.172	0.37248	0.31	0.163	0.7309	0.3023	0.2528	0.2367
	GeoPromptFusion (GPT-4o mini)	0.103	0.289	0.138	0.103	0.164	0.122	0.4409	0.35	0.039	1.1068	0.286	0.1389	0.2644
	GeoResponder (LLaMa)	0.17	0.669	0.275	0.224	0.372	0.28	0.078	0.73	0.529	0.7419	0.2735	0.521	0.2761
	GeoResponder (Mistral)	0.345	0.794	0.493	0.288	0.417	0.34	0.0615	0.94	0.74	0.5656	0.53	0.631	0.4307
	GeoResponder (Qwen)	0.026	0.21	0.056	0.03	0.089	0.047	0.167	0.9	0.047	0.769	0.14	0.16	0.179
	Best GeoResponder vs Best Baseline (%)	0.345	0.794	0.493	0.288	0.417	0.34	0.0615	0.94	0.74	0.5656	0.53	0.631	0.4307
		+50	+17	+54	+115	+57	+98	-83	+169	+354	-23	+75	+150	+52
Paris	LLaMa 3.1 8B	0	0.005	0	0	0.007	0.002	0.829	0.14	0	0.9	0.3719	0.246	0.07
	Mistral 7B v0.3	0	0.003	0	0	0.007	0.001	0.953	0.05	0.004	20	0	0.2289	0.06
	Qwen3 8B	0	0.032	0.001	0.002	0.011	0.003	0.761	0.43	0.002	4.99	0.152	0.0516	0.1
	GeoPromptFusion (LLaMa)	0.022	0.213	0.04	0.073	0.168	0.098	0.76	0.21	0.02	0.736	0.3375	0.257	0.3
	GeoPromptFusion (Mistral)	0.03	0.336	0.06	0.03	0.07	0.039	0.99	0.1	0.02	0.67	0.354	0.2789	0.09
	GeoPromptFusion (Qwen)	0.09	0.558	0.16	0.08	0.236	0.121	0.82	0.43	0.14	0.73	0.256	0.309	0.198
	GeoPromptFusion (GPT-4o mini)	0.032	0.281	0.06	0.022	0.093	0.04	0.48	0.33	0.03	1.06	0.315	0.0954	0.1
	GeoResponder (LLaMa)	0.167	0.945	0.341	0.178	0.449	0.27	0.058	0.82	0.287	0.7519	0.062	0.32	0.1422
	GeoResponder (Mistral)	0.221	0.979	0.407	0.254	0.502	0.348	0.025	0.86	0.531	0.7416	0.336	0.6234	0.499
	GeoResponder (Qwen)	0	0	0	0	0	0	0.159	0.75	0.215	0.7969	0.116	0.3059	0.088
	Best GeoResponder vs Best Baseline (%)	0.221	0.979	0.407	0.254	0.502	0.348	0.025	0.86	0.531	0.7416	0.336	0.6234	0.499
		+146	+75	+154	+217	+113	+188	-95	+100	+279	+11	-10	+102	+66
Manila	LLaMa 3.1 8B	0.004	0.077	0.01	0.001	0.011	0.003	0.52	0.1	0	3.4088	0.058	0	0.0005
	Mistral 7B v0.3	0	0.013	0	0.001	0.007	0.002	0.3	0.02	0	7.7808	0.01	0	0.0005
	Qwen3 8B	0	0.011	0.001	0.001	0.008	0.002	0.503	0.04	0.01	3.3385	0.062	0	0.0388
	GeoPromptFusion (LLaMa)	0.015	0.183	0.026	0.083	0.216	0.113	0.7701	0.09	0.029	0.7205	0.3196	0.0814	0.1645
	GeoPromptFusion (Mistral)	0.023	0.377	0.049	0.031	0.062	0.037	22.2	0.08	0.017	0.6809	0.2375	0.1014	0.1486
	GeoPromptFusion (Qwen)	0.036	0.378	0.068	0.034	0.149	0.059	0.2476	0.3	0.07	0.798	0.2335	0.1348	0.1556
	GeoPromptFusion (GPT-4o mini)	0.009	0.141	0.016	0.009	0.037	0.014	0.1944	0.34	0.016	0.7158	0.339	0.0745	0.1379
	GeoResponder (LLaMa)	0.155	0.837	0.263	0.23	0.451	0.303	0.26	0.87	0.666	0.5303	0.343	0.6356	0.4954
	GeoResponder (Mistral)	0.257	0.977	0.403	0.28	0.478	0.352	0.02	0.95	0.785	0.3376	0.682	0.6839	0.6481
	GeoResponder (Qwen)	0.112	0.848	0.215	0.126	0.363	0.189	0.04	0.85	0.482	0.7147	0.186	0.4889	0.326
	Best GeoResponder vs Best Baseline (%)	0.257	0.977	0.403	0.28	0.478	0.352	0.02	0.95	0.785	0.3376	0.682	0.6839	0.6481
		+614	+158	+493	+237	+121	+212	-90	+179	+1021	-50	+101	+407	+294
New York City	LLaMa 3.1 8B	0.001	0.032	0.003	0.002	0.018	0.005	0.972	0.19	0.007	1.14	0.227	0	0.04
	Mistral 7B v0.3	0.004	0.024	0.007	0.049	0.05	0.049	1.23	0.08	0.006	9	0.015	0	0.0338
	Qwen3 8B	0.002	0.03	0.005	0.019	0.024	0.02	0.747	0.07	0.015	2.5578	0.122	0.01	0.104
	GeoPromptFusion (LLaMa)	0.01	0.2	0.028	0.045	0.169	0.072	0.69	0.1	0.0583	0.788	0.317	0.1474	0.1528
	GeoPromptFusion (Mistral)	0.019	0.277	0.045	0.012	0.07	0.023	0.99	0.05	0.018	0.76	0.323	0.183	0.1373
	GeoPromptFusion (Qwen)	0.035	0.311	0.066	0.025	0.113	0.044	0.86	0.36	0.006	0.648	0.3584	0.2325	0.1557
	GeoPromptFusion (GPT-4o mini)	0.023	0.309	0.053	0.015	0.102	0.032	0.459	0.42	0	0.9	0.29	0	0.1224
	GeoResponder (LLaMa)	0.159	0.888	0.31	0.262	0.546	0.363	0.085	0.7	0.467	0.6696	0.377	0.3922	0.2997
	GeoResponder (Mistral)	0.265	0.979	0.463	0.329	0.612	0.437	0.03	0.91	0.621	0.4615	0.559	0.4861	0.5029
	GeoResponder (Qwen)	0.205	0.885	0.364	0.22	0.524	0.324	0.07	0.89	0.479	0.67	0.316	0.41	0.2501
	Best GeoResponder vs Best Baseline (%)	0.265	0.979	0.463	0.329	0.612	0.437	0.03	0.91	0.621	0.4615	0.559	0.4861	0.5029
		+657	+215	+602	+163	+262	+507	-93	+117	+965	-29	+56	+117	+235

cities, with lower accuracy in denser environments where POI clusters frequently overlap. Road Containment is the most stable task overall, suggesting that reasoning over polygon–polyline relationships is less affected by city scale and density than point-based retrieval. Taken together, these results indicate that non-MCQ accuracy is influenced primarily by density and urban complexity, and that GeoResponder generalizes more reliably for region-based reasoning than for fine-grained point-to-point localization.

6 Conclusion

In this work, we addressed the fundamental deficit of geospatial reasoning in Large Language Models by introducing GeoResponder, a framework that decouples spatial intelligence into a scaffolded curriculum of grounding, reasoning, and constraint-aware retrieval. Our empirical evaluation across heterogeneous urban environments demonstrates that shifting from latent textual correlation to structured topological supervision significantly improves performance.

Crucially, our results establish that internalized spatial representations offer a robust, low-latency complement to brittle agentic workflows, enabling models to resolve complex, constraint-heavy optimization problems directly within their neural weights. Moving forward, we aim to extend this paradigm by integrating multi-modal inputs, such as satellite imagery and real-time sensor streams, paving the way for fully autonomous and resilient geospatial decision support systems.

References

- [1] Pasquale Balsebre, Weiming Huang, and Gao Cong. 2024. LAMP: A Language Model on the Map. arXiv:2403.09059 [cs.CL] <https://arxiv.org/abs/2403.09059>
- [2] Pasquale Balsebre, Weiming Huang, Gao Cong, and Yi Li. 2024. City Foundation Models for Learning General Purpose Representations from OpenStreetMap. In *Proceedings of the 33rd ACM International Conference on Information and Knowledge Management* (Boise, ID, USA) (CIKM '24). Association for Computing Machinery, New York, NY, USA, 87–97. doi:10.1145/3627673.3679662
- [3] Prabin Bhandari, Antonios Anastasopoulos, and Dieter Pfoser. 2023. Are Large Language Models Geospatially Knowledgeable?. In *Proceedings of the 31st ACM International Conference on Advances in Geographic Information Systems (SIGSPATIAL '23)*. ACM, New York, NY, USA. doi:10.1145/3589132.3625625
- [4] Yanchuan Chang, Egemten Tanin, Xin Cao, and Jianzhong Qi. 2023. Spatial Structure-Aware Road Network Embedding via Graph Contrastive Learning. In *EDBT*. 144–156. <https://doi.org/10.48786/edbt.2023.12>
- [5] Anthony G Cohn and Robert E Blackwell. 2024. Evaluating the Ability of Large Language Models to Reason About Cardinal Directions. In *16th International Conference on Spatial Information Theory (COSIT 2024) (Leibniz International Proceedings in Informatics (LIPIcs), Vol. 315)*, Benjamin Adams, Amy L. Griffin, Simon Scheider, and Grant McKenzie (Eds.). Schloss Dagstuhl – Leibniz-Zentrum für Informatik, Dagstuhl, Germany, 28:1–28:9. doi:10.4230/LIPIcs.COSIT.2024.28
- [6] Cheng Deng, Tianhang Zhang, Zhongmou He, Qiyuan Chen, Yuanyuan Shi, Yi Xu, Luoyi Fu, Weinan Zhang, Xinning Wang, Chenghu Zhou, Zhouhan Lin, and Junxian He. 2024. K2: A Foundation Language Model for Geoscience Knowledge Understanding and Utilization. In *Proceedings of the 17th ACM International Conference on Web Search and Data Mining* (Merida, Mexico) (WSDM '24). Association for Computing Machinery, New York, NY, USA, 161–170. doi:10.1145/3616855.3635772
- [7] Ahmed El Fekih Zguir, Ferda Ofli, and Muhammad Imran. 2025. Detecting Actionable Requests and Offers on Social Media During Crises Using LLMs. *Proceedings of the International ISCRAM Conference* (May 2025). doi:10.59297/r9q00255
- [8] Jie Feng, Tianhui Liu, Yuwei Du, Siqi Guo, Yuming Lin, and Yong Li. 2025. CityGPT: Empowering Urban Spatial Cognition of Large Language Models. In *Proceedings of the 31th ACM SIGKDD International Conference on Knowledge Discovery and Data Mining*.
- [9] Wes Gurnee and Max Tegmark. 2024. Language Models Represent Space and Time. arXiv:2310.02207 [cs.LG] <https://arxiv.org/abs/2310.02207>
- [10] Jizhou Huang, Haifeng Wang, Yibo Sun, Yunsheng Shi, Zhengjie Huang, An Zhuo, and Shikun Feng. 2022. ERNIE-GeoL: A Geography-and-Language Pre-trained Model and its Applications in Baidu Maps. In *Proceedings of the 28th ACM SIGKDD Conference on Knowledge Discovery and Data Mining* (Washington DC, USA) (KDD '22). Association for Computing Machinery, New York, NY, USA, 3029–3039. doi:10.1145/3534678.3539021
- [11] Yuhuan Ji, Song Gao, Ying Nie, Ivan Majić, and Krzysztof Janowicz. 2025. Foundation models for geospatial reasoning: assessing the capabilities of large language models in understanding geometries and topological spatial relations. *International Journal of Geographical Information Science* (June 2025), 1–38. doi:10.1080/13658816.2025.2511227
- [12] Yuhuan Ji, Song Gao, Ying Nie, Ivan Majić, and Krzysztof Janowicz. 2025. Foundation models for geospatial reasoning: assessing the capabilities of large language models in understanding geometries and topological spatial relations. *International Journal of Geographical Information Science* 0, 0 (2025), 1–38. arXiv:<https://doi.org/10.1080/13658816.2025.2511227> doi:10.1080/13658816.2025.2511227
- [13] Yue Jiang, Qin Chao, Yile Chen, Xiucheng Li, Shuai Liu, and Gao Cong. 2024. UrbanLLM: Autonomous Urban Activity Planning and Management with Large Language Models. In *Findings of the Association for Computational Linguistics: EMNLP 2024*. 1810–1825. doi:10.18653/v1/2024.findings-emnlp.98
- [14] Pirhossein Kolivand, Peyman Saberian, Mozghan Tanhapour, Fereshteh Karimi, Sharareh Rostam Niakan Kalhori, Zohreh Javanmard, Soroush Heydari, Seyed Saeid Hoseini Talari, Seyed Mohsen Laal Mousavi, Maryam Alidadi, Mahnaz Ahmadi, and Seyed Mohammad Ayyoubzadeh. 2024. A systematic review of Earthquake Early Warning (EEW) systems based on Artificial Intelligence. *Earth Science Informatics* 17, 2 (April 2024), 957–984. doi:10.1007/s12145-024-01253-2
- [15] Zekun Li, Jina Kim, Yao-Yi Chiang, and Muhao Chen. 2022. SpaBERT: A Pre-trained Language Model from Geographic Data for Geo-Entity Representation. arXiv:2210.12213 [cs.CL] <https://arxiv.org/abs/2210.12213>
- [16] Zekun Li, Wenxuan Zhou, Yao-Yi Chiang, and Muhao Chen. 2023. GeoLM: Empowering Language Models for Geospatially Grounded Language Understanding. arXiv:2310.14478 [cs.CL] <https://arxiv.org/abs/2310.14478>
- [17] Rohin Manvi, Samar Khanna, Gengchen Mai, Marshall Burke, David B. Lobell, and Stefano Ermon. 2024. GeoLLM: Extracting Geospatial Knowledge from Large Language Models. In *The Twelfth International Conference on Learning Representations*. <https://openreview.net/forum?id=TqL2xBwXP3>
- [18] Grey Nearing, Deborah Cohen, Vusumuzi Dube, Martin Gauch, Oren Gilon, Shaun Harrigan, Avinatan Hassidim, Daniel Klotz, Frederik Kratzert, Asher Metzger, Sella Nevo, Florian Pappenberger, Christel Prudhomme, Guy Shalev, Shlomo Shenzis, Tadele Yednkachw Tekalign, Dana Weitzner, and Yossi Matias. 2024. Global prediction of extreme floods in ungauged watersheds. *Nature* 627, 8004 (March 2024), 559–563. doi:10.1038/s41586-024-07145-1
- [19] Jonathan Roberts, Timo Lüddecke, Sowmen Das, Kai Han, and Samuel Albanie. 2023. GPT4GEO: How a Language Model Sees the World's Geography. arXiv:2306.00020 [cs.CL] <https://arxiv.org/abs/2306.00020>
- [20] Harikesh Singh, Li-Minn Ang, and Sanjeev Kumar Srivastava. 2025. Active wildfire detection via satellite imagery and machine learning: an empirical investigation of Australian wildfires. *Natural Hazards* 121, 8 (March 2025), 9777–9800. doi:10.1007/s11069-025-07163-w
- [21] Eren Unlu. 2023. Chatmap: Large Language Model Interaction with Cartographic Data. arXiv:2310.01429 [cs.CL] <https://arxiv.org/abs/2310.01429>
- [22] WFP, Google research. 2024. SKAI: Unleashing the Power of Artificial Intelligence to Revolutionize Disaster Response and Humanitarian Aid. <https://innovation.wfp.org/project/SKAI>.
- [23] Yifan Zhang, Cheng Wei, Zhengting He, and Wenhao Yu. 2024. GeoGPT: An assistant for understanding and processing geospatial tasks. *International Journal of Applied Earth Observation and Geoinformation* 131 (2024), 103976. doi:10.1016/j.jag.2024.103976

A Ablation

Figure 5 summarizes the contribution of each geospatial representation by removing one representation at a time and measuring the resulting drop in the average downstream performance. Every ablation leads to a decline, confirming that all representations contribute meaningfully to the model's overall geospatial capability.

The largest degradation occurs when removing the *network topology* representation, with a drop of approximately 16.6%. This is expected: network topology constitutes the largest portion of the training data (Table 3) and encodes fundamental structural constraints of the road graph. Without it, the model loses access to essential connectivity cues that support routing, adjacency reasoning, and multi-hop spatial inference.

Other representations also produce notable drops. Removing *Road Containment*, *Directional Nearest Road*, or *POI Containment* reduces performance by 3–4%, reflecting their importance for region-based and directional reasoning. Tasks tied to point retrieval, such as POI Lookup, Reverse POI Lookup, and Direction Inference, yield smaller but still consistent declines. Even Category Scan, the least impactful ablation, results in a measurable drop, demonstrating that each representation contributes a unique signal.

Overall, the ablation results show that GeoResponder benefits from the complementary structure of all representations. No single representation alone is sufficient; instead, strong performance emerges from combining topological, directional, containment, and retrieval-based cues into a unified geospatial training framework.

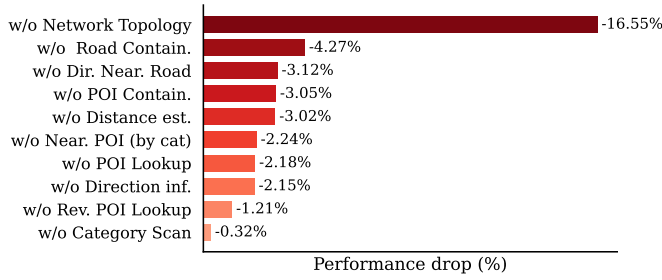


Figure 5: Ablation study showing the average performance drop when individual representations are removed. Bars indicate the reduction in the unified metric (average of all downstream tasks).

B Extra Cities Information

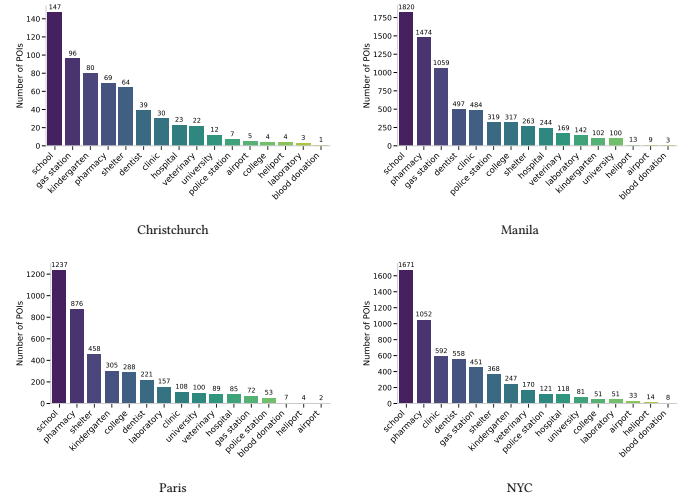


Figure 7: POI category distributions across the four cities.

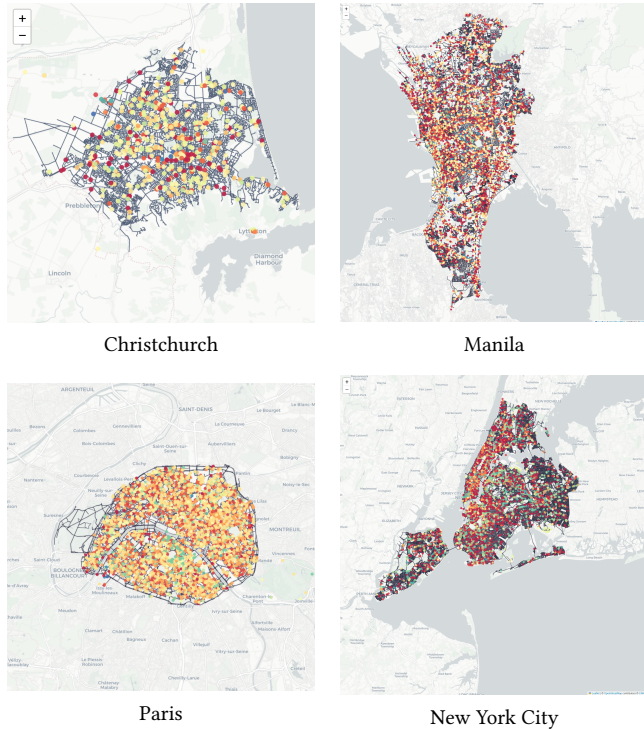


Figure 6: Maps of the four benchmark cities with grey roads and colored POI dots, where each color indicates a different POI category.

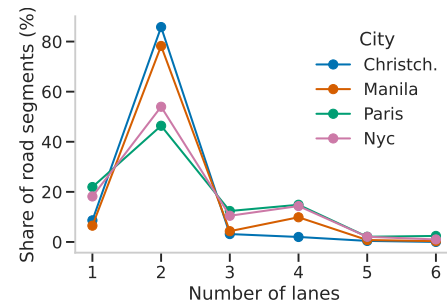


Figure 8: Lanes distribution across the four cities.

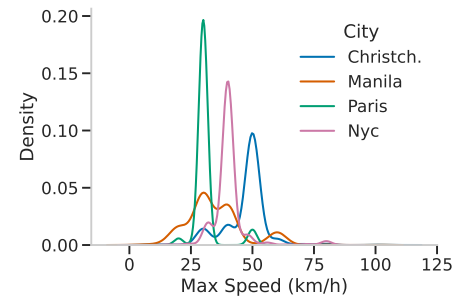


Figure 9: Maxspeed distribution across the four cities.

C Example Prompts

OOD Task: Nearest Road (POI)

Context. After a major storm in Paris, field teams must quickly determine access routes for response units. Staff located at the point of interest (POI) Hôpital Saint-Louis need to identify the nearest road so that responders can plan an approach path.

Instruction. This is a multiple choice question. Identify which road is closest to the given POI. Answer using only one letter from the provided options.

Figure 10: Example OOD prompt for the Nearest Road (POI) task.